Praca oryginalna *Original paper*

The protective effect of dihydromyricetin against LPS-induced liver and intestinal injury in mice*

YING LI, HAO XU, XIAOYU WU, HAOYUAN ZHAI, YUE WU, XIN WANG

College of Animal Science and Veterinary Medicine, Heilongjiang Bayi Agricultural University, Daqing 163319, China

Received 30.05.2026 *Accepted 08.07.2026*

Li Y., Xu H., Wu X. Y., Zhai H. Y., Wu Y., Wang X.

The protective effect of dihydromyricetin against LPS-induced liver and intestinal injury in mice

Summary

Objective: This study was conducted to examine the protective effects of dihydromyricetin (DHM) against LPS-induced hepatic and intestinal injury in mice. Methods: Mice were divided into control, LPS, and DHM (100, 200, 400 mg/kg) groups. DHM was given by gavage for 14 days before LPS injection. LPS was injected intraperitoneally to establish injury models. Serum biochemical indexes, hepatic antioxidant indicators, and histopathology with semi-quantitative scoring were assessed. Results: LPS increased serum AST, ALT, DAO, and D-lactate, elevated hepatic MDA, decreased T-SOD, GSH-Px, and T-AOC, and caused severe intestinal and hepatic damage. Medium and high doses of DHM reversed the above changes. Conclusion: DHM protects against LPS-induced hepatointestinal injury through intestinal barrier preservation and antioxidant enhancement, suggesting its potential as a natural feed additive.

Keywords: dihydromyricetin, LPS, liver and intestinal injury, antioxidant

Early weaning is widely applied in pig production to improve sow productivity and reduce pathogen transmission (12). However, it disturbs redox homeostasis and induces excessive production of reactive oxygen species (ROS) in piglets (7). Excess ROS damage hepatocytes and intestinal epithelium and activate pro-inflammatory pathways (e.g., MAPK), compromising hepatic and intestinal functions (9). Despite these effects, the mechanisms of hepatointestinal injury remain unclear, and effective interventions are still being explored. Dihydromyricetin (DHM), a flavonoid from *Ampelopsis grossedentata*, scavenges ROS, restores redox homeostasis, and inhibits TLR4/NF-κB to reduce inflammation (11, 18). It also regulates glucose and lipid metabolism, alleviates liver injury, and strengthens the intestinal barrier (4, 8). Although DHM has been extensively investigated in medical fields, its potential as a green feed additive in livestock has attracted interest only recently. Given the practical and ethical constraints of mechanistic studies in swine, we established a LPS-induced hepatointestinal injury model in mice to evaluate the protective effects of DHM on the gut-liver axis. These findings provide experimental evidence for the protective role of DHM against hepatointestinal injury and may inform future studies in weaned piglets.

Material and methods

Escherichia coli LPS (serotype 055:B5) was purchased from Sigma-Aldrich (St. Louis, MO, USA). Dihydromyricetin (DHM, purity > 98.0%) was obtained from Shanghai Winherb Medical Science Co., Ltd. (Shanghai, China). Male Kunming mice were obtained from the Animal Experiment Center of Harbin Medical University (Daqing, China) with the production license SYXK (Hei) 2014-005.

Male mice (18-22 g) were housed at 22-24°C with a 12-h light/dark cycle. All animals had free access to food and water. After one week of acclimatization, the mice were randomly divided into five groups (n = 10 per group): control group, LPS group, DHM-L group (100 mg/kg), DHM-M group (200 mg/kg), and DHM-H group (400 mg/kg). Mice in the control and LPS groups were intragastrically given 0.2 mL of 0.9% saline once daily for 14 consecutive days. The DHM-treated groups received an equal volume of DHM suspension at different doses (100, 200 or 400 mg/kg) over the same period (17). After the final administration, all mice were fasted for 6 h. Then, all mice except controls were injected intraperitoneally with 10 mg/kg LPS, 0.2 mL, while the controls were given the same volume of sterile saline (5). All animal experiments were approved by the Animal Ethics Committee of Heilongjiang Bayi Agricultural University (Approval No. DWKJXY202589).

* Funding Statement: This article is supported by the Heilongjiang Postdoctoral Fund, grant number LBH-Z21193; Research Initiation Plan for Academically Accomplished and Introduced Talents at Heilongjiang Bayi Agricultural University, grant number XYB201915; „Three-Tier" Basic Incubation Project of Heilongjiang Bayi Agricultural University, grant number ZRCPY202310.

Six hours after LPS challenge, blood samples were collected from the retro-orbital venous plexus. Whole blood was kept at room temperature for 2 h and then centrifuged at 3,500 rpm for 10 min to separate serum. After blood sampling, all mice were euthanized by cervical dislocation. The liver, jejunum, and ileum were immediately isolated and rinsed with pre-cooled 0.9% sterile saline. Partial tissue samples were fixed in 10% neutral buffered formalin for hematoxylin and eosin (H&E) staining. The remaining liver tissue was homogenized in 0.9% saline to prepare 10% (w/v) tissue homogenate, followed by centrifugation at 3,500 rpm for 15 min. The supernatant obtained was collected and stored at –80°C for subsequent detection.

Tissues were fixed in 10% neutral buffered formalin for at least 24 h, then dehydrated, cleared in xylene, and embedded in paraffin. The tissue blocks were cut into 4 µm transverse sections, mounted on glass slides, and stained with H&E. Finally, the sections were coverslipped using mounting medium. Pathological changes were observed and imaged under an optical microscope (Nikon E100, Japan). For semi-quantitative assessment of intestinal injury, five random fields per section were examined at 100 × magnification, and each field was scored using a 0-4 scale: 0 = normal mucosa, 1 = injury of the villus tip, 2 = partial loss of villi, 3 = severe injury of the submucosa, 4 = complete necrosis (13). The average score was calculated for each sample. Liver injury was assessed based on the degree of hepatic lobule destruction, inflammatory cell infiltration, hemorrhage, and hepatocyte necrosis (2). Each parameter was scored on a 0-4 scale according to the percentage of the affected area per field at 400 × magnification: 0 = no damage, 1 = 1%-25%, 2 = 26%-50%, 3 = 51%-75%, 4 = 76%-100% as described previously (2).

Serum activities of ALT, AST, and DAO, as well as D-lactic acid content, were determined using assay kits purchased from Shanghai Enzyme-Linked Biotechnology Co., Ltd. All procedures were performed according to the manufacturer's instructions.

Hepatic levels of MDA and GSH, as well as the activities of GSH-Px and T-SOD, were measured using an assay kit from the Nanjing Jiancheng Institute of Biotechnology (China) in accordance with the manufacturer's instructions.

All data were analyzed by one-way analysis of variance (ANOVA) followed by Duncan's multiple range test using the SPSS 19.0 software. The results were presented as mean ± standard deviation (SD). A $p < 0.05$ was defined as statistically significant, and $p < 0.01$ was defined as highly significant.

Results and discussion

As shown in Figure 1B, serum DAO and D-lactate were markedly elevated in the LPS group relative to the control group ($p < 0.05$). Both indicators declined in the DHM-treated mice compared with the LPS group, and significant differences were found in the DHM-M and DHM-H groups ($p < 0.01$). These results suggested that DHM could relieve LPS-induced intestinal injury.

As shown in Figure 1C, serum ALT and AST were significantly higher in the LPS group than in the control group ($p < 0.01$). All three DHM treatment groups

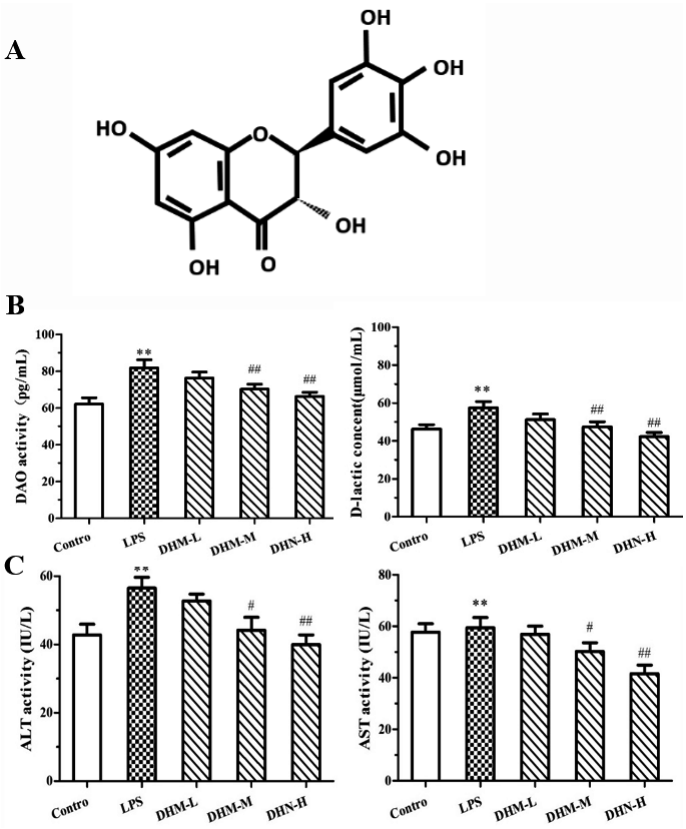

Fig. 1. Determination of injury-specific indicators. (A) Chemical structure of dihydromyricetin; (B) Effects of DHM on serum DAO and D-lactate levels; (C) Effects of DHM on serum ALT and AST levels

Explanations: *$p < 0.05$, **$p < 0.01$ compared to the control group; #$p < 0.05$, ##$p < 0.01$ compared to the LPS group.

presented reduced ALT and AST activities. The effects were more pronounced in the DHM-M and DHM-H groups, with significant differences versus the LPS group ($p < 0.05$ and $p < 0.01$, respectively). These data demonstrated that DHM could downregulate serum ALT and AST activities and mitigate LPS-induced hepatic injury.

Representative H&E-stained histopathological images of the jejunum and ileum are displayed in Figure 2A and 2E. In the control group, the jejunal and ileal mucosa showed regular arrangement. Intestinal villi and crypt structures were intact, with abundant goblet cells. No inflammatory cell infiltration was observed, and the layered structure of the intestinal wall remained complete and clear. The LPS group developed severe intestinal lesions, including congestion in the lamina propria and submucosa, villous ablation, mucosal vasodilation, epithelial debris, and fibrinous exudate in the intestinal lumen, neutrophil accumulation within crypts, and massive infiltration of lymphocytes and plasma cells in the crypt base. Compared with the LPS group, the DHM-M and DHM-H groups exhibited well-organized mucosa, nearly intact intestinal epithelium and obviously decreased inflammatory infiltration in the crypt base. For the ileum, DHM-L only exerted a mild protective effect. DHM-M and DHM-H

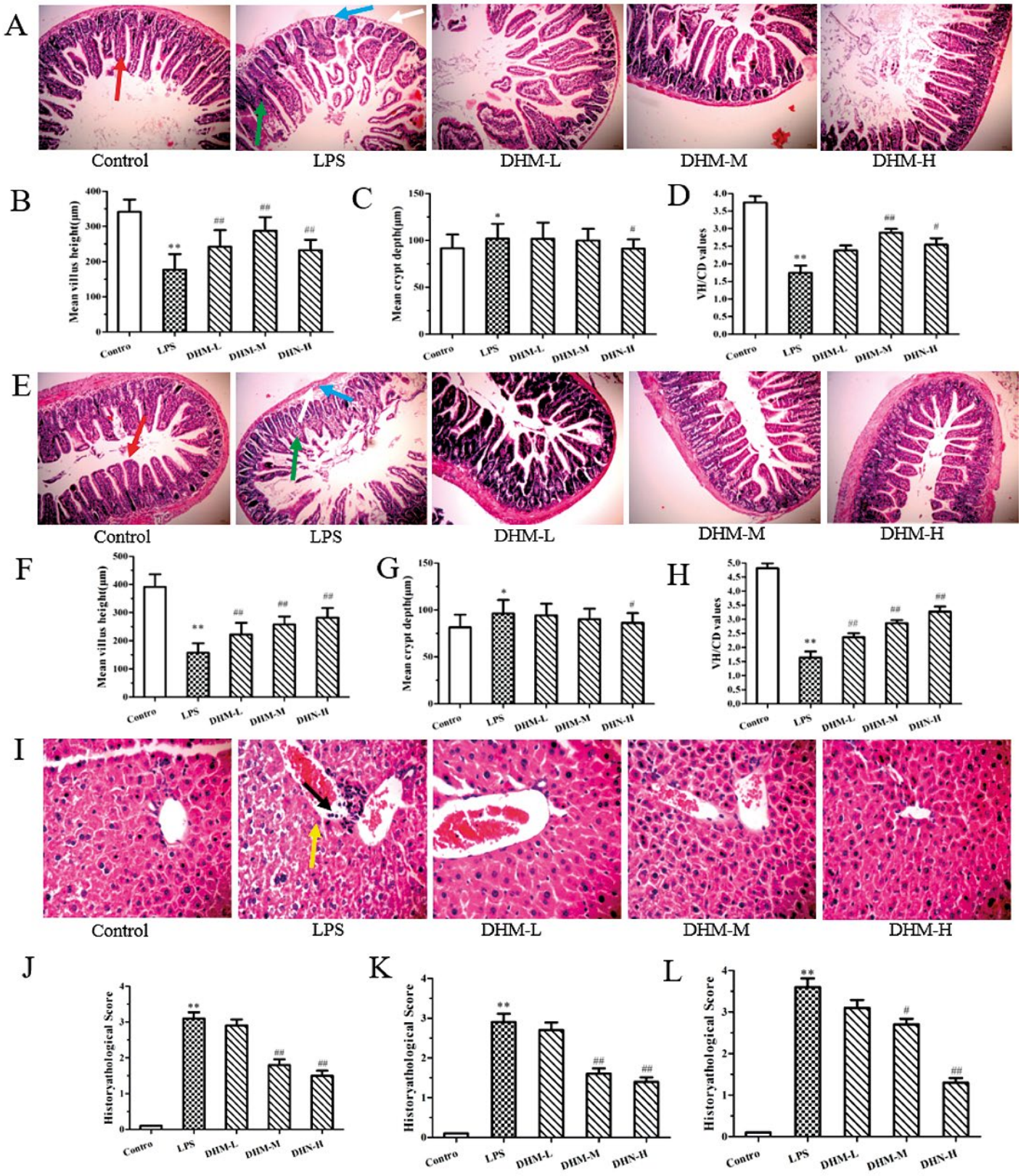

Fig. 2. Histopathological analysis. (A) Representative H&E staining of jejunum tissues; (B) Mean villus height of jejunum; (C) Mean crypt depth of jejunum; (D) Ratio of villus height to crypt depth of jejunum; (E) Representative H&E staining of ileum tissues; (F) Mean villus height of ileum; (G) Mean crypt depth of ileum; (H) Ratio of villus height to crypt depth of ileum; (I) Representative H&E staining of liver tissues; (J) Histopathological score of jejunum tissues; (K) Histopathological score of ileum tissues; (L) Histopathological score of liver tissues

Explanations: red arrows – goblet cells; green arrows – neutrophils; blue arrows – lymphocytes; white arrows – plasma cells; black arrows – lymphocytes; yellow arrows – steatosis

achieved much better outcomes, though a small number of inflammatory cells were still detectable in the DHM-M group.

Quantitative analysis of intestinal morphological parameters is presented in Figures 2B-D and 2F-H. Compared with the control group, the LPS group had lower villus height and villus height/crypt depth ratio ($p < 0.01$), as well as increased crypt depth in both jejunum and ileum ($p < 0.05$). Medium- and high-dose DHM remarkably remedied LPS-induced villus shortening in the two intestinal segments ($p < 0.01$). High-dose DHM also effectively reduced crypt depth ($p < 0.05$). Moreover, both DHM-M and DHM-H markedly increased the villus height/crypt depth ratio ($p < 0.01$). Collectively, DHM reversed intestinal structural damage in the LPS-challenged mice in a dose-dependent manner.

The histopathological micrographs of liver tissues measured by H□E staining are shown in Figure 2I. In the control group, the structure of hepatic lobules was complete, with regularly arranged hepatic cords and normal hepatocyte morphology. In the LPS group, hepatic lobule architecture became blurred with indistinct boundaries and disorganized hepatic cords. Hepatocytes exhibited typical necrotic changes, including pyknosis, karyorrhexis, and karyolysis, accompanied by cytoplasmic lysis, membrane rupture, and steatosis. Hepatic sinusoids were severely dilated and congested, and obvious lymphocyte infiltration was observed around the central vein. Compared with the LPS group, the low-dose DHM group still showed blurred hepatic lobules and disorganized hepatic cords, but the pathological changes were partially reversed. Erythrocyte and inflammatory cell infiltrations in the central vein were alleviated. In the DHM-M group, hepatic lobule structure and hepatic cord arrangement recovered obviously, while sinusoidal dilation and inflammatory infiltration decreased. In the DHM-H group, hepatic histomorphology was largely restored to the normal state similar to that in the control group, with only mild hemorrhage in the central vein.

As shown in Figure 2J-K, semi-quantitative histopathological scoring revealed that the LPS group had significantly higher injury scores than the control group in the jejunum, ileum, and liver ($p < 0.01$). DHM treatment dose-dependently reduced the scores in the DHM-M and DHM-H groups ($p < 0.05$ or $p < 0.01$).

As summarized in Table 1, compared with the control group, the LPS group presented remarkable reductions in hepatic GSH-Px, T-AOC, and T-SOD activities, whereas MDA content was markedly elevated ($p < 0.01$). Relative to the LPS group, all DHM treatment groups had increased antioxidant indicators and decreased MDA levels ($p < 0.05$, $p < 0.01$). These findings indicate that DHM could relieve hepatic injury and oxidative stress, thereby exerting a protective effect on the liver.

The gut-liver axis provides a framework for understanding the protective effects of DHM in both the intestine and liver. Under physiological conditions, the intestinal barrier prevents luminal LPS from reaching the liver by portal circulation (1). Evidence of intestinal barrier compromise in LPS-treated mice included elevated serum DAO and D-lactate levels, villus shortening, and crypt hyperplasia. Consequently, LPS translocates to the liver, where it activates TLR4/NF-κB signaling and triggers local inflammatory and oxidative responses (6). This mechanistic sequence aligns with our concurrent observation of hepatic damage (elevated ALT/AST and histopathological changes) alongside intestinal injury. DHM administration, particularly at medium and high doses, attenuated both intestinal and hepatic lesions. This was reflected by restored villus height/crypt depth ratio, reduced serum markers of intestinal barrier dysfunction, and lowered transaminase activities. The concomitant protection suggests that DHM may break the vicious cycle of gut-derived endotoxemia and hepatic inflammation by preserving intestinal structural integrity, thereby limiting LPS translocation to the liver. In addition, DHM may act directly on hepatocytes to enhance antioxidant capacity, as suggested by the elevated hepatic SOD/GSH-px activities in DHM-treated groups. Whether the intestinal and hepatic effects are causally linked or occur independently cannot be determined from the current data and remains a key question for future research.

LPS induces oxidative stress via NADPH oxidase and mitochondrial dysfunction, causing lipid peroxidation and cell injury (10, 14). The LPS-challenged mice showed elevated hepatic MDA and reduced SOD, GSH-Px, and T-AOC, confirming the occurrence of severe oxidative damage. DHM dose-dependently reversed these changes, which suggests that it protects the liver by preserving endogenous antioxidant enzyme activity rather than by directly scavenging ROS. Among the three doses tested, the medium and

Tab. 1. Effects of DHM on biochemical indices and oxidative stress in the mouse liver

Group	MDA (nmol/mg protein)	GSH-Px (U/mg protein)	T-AOC (U/mg protein)	T-SOD (U/mg protein)
Control group	1.55 ± 0.36	84.89 ± 13.38	0.50 ± 0.11	194.74 ± 19.18
LPS group	1.77 ± 0.20**	59.10 ± 25.61**	0.38 ± 0.05**	183.10 ± 13.67**
DHM-L group	1.64 ± 0.46#	67.11 ± 11.46#	0.42 ± 0.08##	188.80 ± 15.10#
DHM-M group	1.40 ± 0.25##	78.00 ± 9.39##	0.45 ± 0.09##	190.32 ± 17.50##
DHM-H group	1.33 ± 0.17##	80.87 ± 22.42##	0.48 ± 0.04##	195.86 ± 12.35##

Explanations: *$p < 0.05$, **$p < 0.01$ compared to the control group; #$p < 0.05$, ##$p < 0.01$ compared to the LPS group.

high doses (200 and 400 mg/kg) produced comparable effects on most oxidative parameters, implying that a threshold effect may exist beyond which higher DHM concentrations yield diminishing returns.

Mechanistically, DHM inhibits NLRP3 inflammasome activation, reduces pro-inflammatory cytokines, and upregulates intestinal tight junction proteins (15, 16). Consistent with these findings, our study showed that DHM alleviated jejunal and ileal morphological damage, reduced inflammatory infiltration, and restored villus height and villus-to-crypt ratio. Meanwhile, DHM significantly decreased serum DAO and D-lactate levels, confirming improved intestinal barrier function. Notably, the medium (200 mg/kg) and high (400 mg/kg) doses produced largely comparable protective effects, implying that an optimal dose range may exist beyond which additional DHM offers limited benefits. These findings support the potential of DHM as a candidate feed additive for preventing endotoxemia-related acute hepatic and intestinal injury.

Several limitations of the present study should be acknowledged. The study was performed in male mice, and the 6 h time point captures only acute responses, leaving chronic effects unexplored. The use of a murine model, while advantageous for controlled mechanistic evaluation, inevitably raises questions about extrapolation to pigs, especially given species differences in drug handling and gut ecology. Finally, the preventive dosing schedule, although appropriate for proof-of-concept studies, may not mirror the therapeutic use in veterinary practice. These caveats underscore the need for future investigations in swine, with a focus on clinically relevant endpoints and long-term safety.

References

1. *Araujo E. M. de, Torres U. S., Racy D. J., Torres L. R., Chojniak R., D'Ippolito G.*: The "streamline phenomenon" of the portal vein flow and its influence on liver involvement by gastrointestinal diseases: current concepts and imaging-based review. Abdominal Radiology 2020, 45 (2), 403-415.
2. *Baranova I. N., Souza A. C. P., Bocharov A. V., Vishnyakova T. G., Hu X. Z., Vaisman B. L., Amar M. J., Chen Z. G., Kost Y., Remaley A., Patterson A. P., Yuen P. S. T., Star R. A., Eggerman T. L.*: Human SR-BI and SR-BII potentiate lipopolysaccharide-induced inflammation and acute liver and kidney injury in mice. Journal of Immunology 2016, 196 (7), 3135-3147.
3. *Chang Y. C., Jiang X. R., Ji Z. H., Gong Y. C., Fan X. N., Hao B. L., Yuan L., Muhammad I., Li R., Li C. W., Liu F. P.*: Dihydromyricetin suppresses lipopolysaccharide-induced intestinal injury through reducing reactive oxygen species generation and NOD-like receptor pyrin domain containing 3 inflammasome activation. Journal of Animal Physiology and Animal Nutrition 2025, 109 (2), 610-622.
4. *Chen X. L., He X. L., Du X. Y.,Huang Z. Q., Jia G., Zhao H.*: Dihydromyricetin attenuates lipopolysaccharide-induced intestinal injury in weaned piglets by regulating oxidative stress and inhibiting NLRP3 inflammasome. Journal of Animal Science 2025, 103: skaf114.
5. *Dou X. N., Qiao L., Song X. F., Chang J. J., Zeng X. N., Zhu L. X., Deng T. J., Yang G., Xu C. L.*: Biogenic selenium nanoparticles alleviate intestinal barrier injury in mice through TBC1D15/Fis1/Rab7 pathway. Biomedicine & Pharmacotherapy 2024, 175, 116740.
6. *Jain H., Kumar A., Almousa S., Mishra S., Langsten K. L., Kim S., Sharma M., Su Y. X., Singh S., Kerr B. A., Deep G.*: Characterisation of LPS+ bacterial extracellular vesicles along the gut-hepatic portal vein-liver axis. Journal of Extracellular Vesicles 2024, 13 (7), e12474.
7. *Ji X., Tang Z. Q., Zhang F., Zhou F.*: Dietary taurine supplementation counteracts deoxynivalenol-induced liver injury via alleviating oxidative stress, mitochondrial dysfunction, apoptosis, and inflammation in piglets. Ecotoxicology and Environmental Safety 2023, 253, 114705.
8. *Jia L. N., Liu J. R., Ji Z. H., Yuan L., Gong Y. C., Jiang X. R., Fan X. N., Li C. W., Li R., Wang H. R., Liu F. P.*: Dihydromyricetin attenuates LPS-induced liver injury in chicks through the JNK signaling pathway. Research in Veterinary Science 2026, 205, 106165.
9. *Jiang Z. P., Yang M. Z., Su W. F., Mei L., Li Y. Q., Guo Y. G., Li Y. Y., Liang Q. F., Yang B., Huang Z. Y., Wang Y. Z.*: Probiotics in piglet: from gut health to pathogen defense mechanisms. Frontiers in Immunology 2024, 15, 1468873.
10. *Kouki A., Ferjani W., Ghanem-Boughanmi N., Ben-Attia M., Dang P. M., Souli A., EI-Benna J.*: The NADPH oxidase inhibitors apocynin and diphenyleneiodonium protect rats from LPS-induced pulmonary inflammation. Antioxidants 2023, 12 (3), 770.
11. *Matouk A. I., Awad E. M., El-Tahawy N. F. G., EI-Sheikh A. A. K., Was S.*: Dihydromyricetin alleviates methotrexate-induced hepatotoxicity via suppressing the TLR4/NF-κB pathway and NLRP3 inflammasome/caspase 1 axis. Biomedicine & Pharmacotherapy 2022, 155, 113752.
12. *Saladrigas-García M., D'Angelo M., Ko H. K., Nolis P., Ramayo-Caldas Y., Folch J. M., Llonch P., Solà-Oriol D., Pérez J. F., Martín-Orúe S. M.*: Understanding host-microbiota interactions in the commercial piglet around weaning. Scientific Reports 2021, 11 (1), 23488.
13. *Tayman C., Uckan D., Kilic E., Ulus A. T., Tonbul A., Hirfanoglu I. M., Helvacioglu F., Haltas H., Koseoglu B., Tatli M. M.*: Mesenchymal stem cell therapy in necrotizing enterocolitis: a rat study. Pediatric Research 2011, 70 (5), 489-494.
14. *Wang L. L., Deng Z. F., Huang J. Y., Li T. Y., Jiang J., Wang W., Sun Y., Deng Y. Q.*: Zearalenone-induced hepatointestinal toxicity in laying hens: unveiling the role of gut microbiota and fecal metabolites. Poultry Science 2024, 103 (11), 104221.
15. *Wu D. S., Fan X. N., Ji Z. H., Jiang X. R., Wang S. B., Ren Y. N., Li C. W., Chang Y. C., Liu F. P.*: Dihydromyricetin ameliorates Salmonella enteritidis-induced pyroptosis and intestinal damage in chickens via modulating NLRP3 inflammasome. Journal of Ethnopharmacology 2026, 362, 121382.
16. *Xie K. H., Qi J. W., Deng L. L., Yu B., Luo Y. H., Huang Z. Q., Mao X. B., Yu J., Zheng P., Yan H., Li Y., Li H., He J.*: Protective effect of dihydromyricetin on intestinal epithelium in weaned pigs upon enterotoxigenic Escherichia coli challenge. International Immunopharmacology 2024, 140, 112806.
17. *Xu Z. M., Zhang M. J., Zhang X., Han H. R., Ye W. F., Chen Z. J., Lv Z. S., Liu Y., Liu Z. Y.,Gong J. G., Zhu B., Zhou S. H., Zhu R. Z., Tao C., Zhang G. S., Yan X.*: Dihydromyricetin protects against cisplatin-induced renal injury and mitochondria-mediated apoptosis via the EGFR/HSP27/STAT3 signaling pathway. Renal Failure 2025, 47 (1), 2490202.
18. *Yang Y., Qiu W., Xiao J. Y., Sun J., Ren X., Jiang L. X.*: Dihydromyricetin ameliorates hepatic steatosis and insulin resistance via AMPK/PGC-1α and PPARα-mediated autophagy pathway. Journal of Translational Medicine 2024, 22 (1), 309.

First author: Ying Li, PhD, College of Animal Science and Veterinary Medicine, Heilongjiang Bayi Agricultural University, No. 5 Xinfeng Road, Daqing 163319, China; e-mail: liying980980@126.com